SEMIANALYTIC THEORY OF MOTION FOR LEO SATELLITES UNDER AIR DRAG

A. Bezděk

Astronomical Institute, Academy of Sciences of the Czech Republic,
Fričova 298, 251 65 Ondřejov, Czech Republic, E-mail: bezdek@asu.cas.cz

ABSTRACT

The presented semianalytic theory focuses on the long-term evolution of the LEO satellites motion, with the TD/TD88 model of the total density as a key ingredient. Besides, the theory takes into account the main geopotential perturbations, for satellites with low eccentricity and/or inclination, nonsingular elements are used. An interesting feature of the theory is its computational speed (e.g. the 10-year propagation takes 5.5 s on a PC with Intel Celeron 1.7 GHz), while considering major physical conditions that strongly influence the thermospheric density (solar flux, geomagnetic activity, diurnal and seasonal variations, geographic latitude). The online calculation as well as the code are available on the Internet.

The theory has been tested against the real world data of several spherical satellites. For the lifetime prediction accuracy estimate of the theory, we used a confidential interval based on the uncertainty in the drag coefficient C_D, while taking the measured values of the solar flux and geomagnetic index. The modelled long-term behaviour of the orbital elements is in reasonably good agreement with the data, the computed lifetimes fall within the C_D-induced confidential intervals, typical error in the mean lifetime prediction being a few percent.

The tests showed that – provided one appropriately models the solar and geomagnetic activity – the theory may be used in the areas where one needs a quick orbital propagator for LEO objects influenced by air drag (mission planning, lifetime prediction, space debris dynamics). As an example, we will show the mission planning and the medium-term prediction of the motion for the MIMOSA satellite.

1 ORBITAL DYNAMICS AT LEO HEIGHTS

The motion of a spacecraft in low Earth orbit (LEO) is influenced mainly by gravity and air drag. To predict the orbital behaviour of the body one must choose a model for each of these forces and a method for solving the differential equations of motion, often the decision on the first question will limit the options of the second and vice versa. The models of the gravitational field are of the same basic mathematical structure, and the gravitational part of the equations of motion will be essentially the same for different gravitational fields [1].

In case of the thermosphere the situation is different – in orbital dynamics the semiempirical models (e.g. Jacchia, MSIS or DTM model series, for references see [2]) are used for the most detailed description of the neutral thermosphere, and oversimplified analytical models for a quick analytical computation. The semiempirical models are based on the physical assumptions, some of which rather simplified (e.g. the diffusive equilibrium of atmospheric components), and take into account the dynamic variation of the thermosphere due to solar activity. The numerical quadrature of the diffusion equations can be very CPU demanding, so several mathematically efficient approximations to the semiempirical models have been proposed [e.g. 3, 4]. The analytical models of the thermosphere are usually based on exponential or power function representation of the total density, sometimes with a refinement e.g. for the Earth oblateness or the altitude dependent scale height [1, 5]. Let us remark that there are also fully physical models of the upper atmosphere (based on the transport equations), but they are too complicated for use in orbital dynamics and show no quantitative advantage over semiempirical models [6].

1.1 Overview of solution methods

Reference [1] distinguishes three mathematical solution techniques for the osculating equations of motion: numerical, semianalytical and analytical. A numerical method applies numerical integration to the osculating differential equations of motion. Both semianalytical and analytical methods analytically transform from the osculating to a mean set of equations. A semianalytical method numerically propagates the mean equations of motion, which are more slowly varying than the osculating ones, thus allowing a much larger time step. The osculating state is obtained through an inverse analytical transformation. This applies to the analytical methods as well, these can integrate the mean equations of motion to readily predict the mean state at a later time. An analytical method goes through an initialization section only once, whereas a semianalytical method must be reinitialized at each integration step.

2 THE STOAG THEORY

The presented theory of motion for LEO satellites may be divided into two parts according to the overview above – the perturbations due to drag are treated semianalytically, those due to the geopotential analytically. The theory originated from the semianalytical theory of motion of an artificial satellite in the Earth atmosphere [7, 8], which was based on the specific formula of the thermospheric total density model TD88 [9–11]. In principle, the model TD88 is analytic (a sum of exponential functions), but by means of an appropriate weighting of the base exponentials it takes into account the physical parameters having influence on the thermospheric density

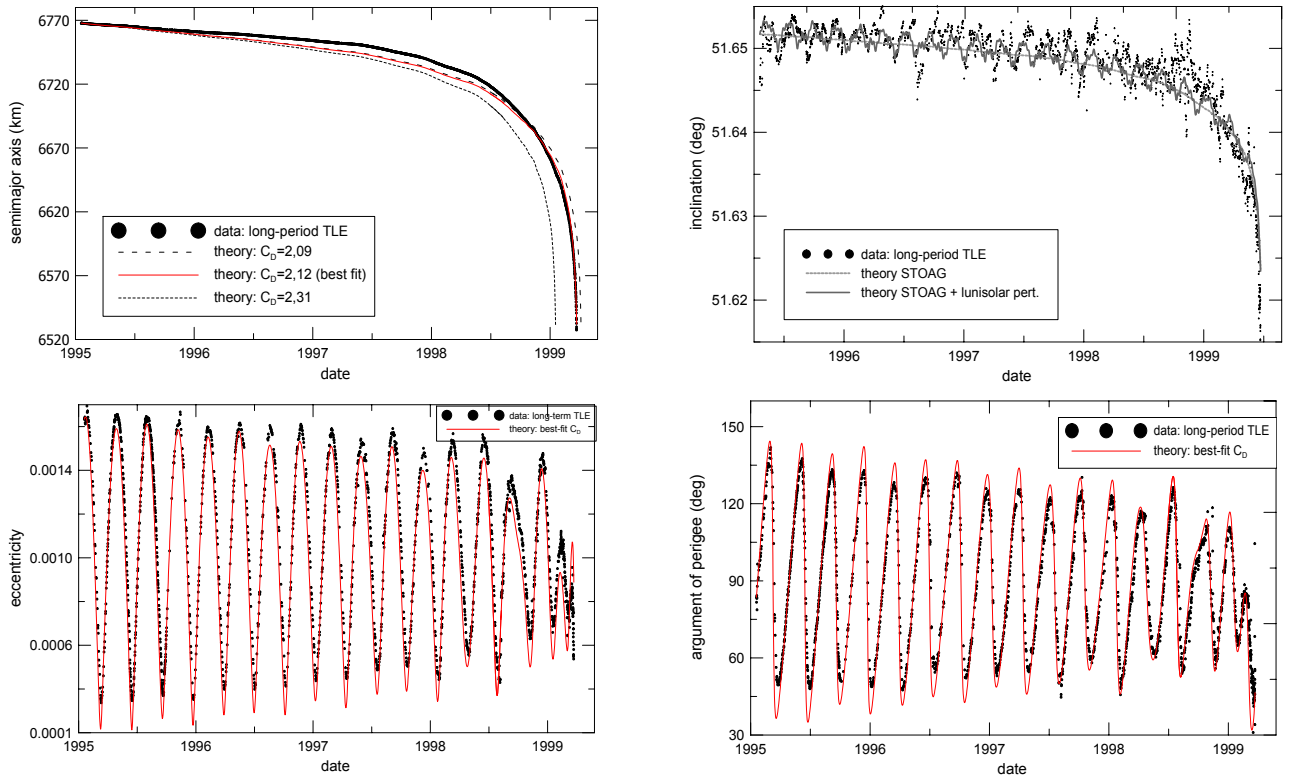

Fig. 1. Long-term evolution of the orbital elements of satellite GFZ-1 (d = 21.5 cm, m = 20.63 kg).

(solar flux, geomagnetic activity, diurnal and seasonal variations, geographic latitude). The TD88's free parameters are adjustable to fit at best the model or real density data (the original version [9–11] employed the DTM-78 model densities [12]), so TD88 may be viewed as a mathematical approximation to virtually any semiempirical model, in a manner similar to the approximations [3, 4] cited above. On the other hand, the structure of TD88 is devised in such a way it that allows the osculating equations of motion to be analytically integrated over one revolution of the satellite [conf. 13], which permits one to use the mean equations of motion. Thus, one revolution of the satellite represents a characteristic time step of the theory, which is also suitable with respect to the typical time scale with which the usual input parameters of the thermospheric density models are measured (daily values of solar flux, three-hour index K_p). For the calculation of the thermospheric density, therefore, the above mentioned reinitialization after each integration step is desirable, as the density variations caused by geomagnetic disturbances or solar flares may reach tens of percent.

The long-period and secular gravitational perturbations of the presented theory depend on the zonal harmonics J_2–J_9 of the geopotential, which we take as constant in time. For their inclusion in the theory – in contrast to the perturbations due to drag – we could use some of the existing methods, so we chose the well-known technique based on the classical analytical results by Brouwer and Kozai summarized in [14], thus generalizing the original work [8], where only the first order secular changes due to J_2 were implemented. In order to test the theory predictions against passive spherical satellites, which often have near-circular orbits, we modified both the drag and gravitational parts of the theory to work in the eccentricity nonsingular elements [for details, see 2]. Compared to the previous version of the presented theory [2], we added the long-period lunisolar perturbations according to [15], taking the orbits of Sun and Moon as circular, in case of Moon with zero inclination.

In what follows, the presented theory of satellite motion comprising both drag and gravitational perturbations will be referred to as the STOAG theory (Semianalytic Theory of mOtion under Air drag and Gravity), when referencing to the long-term perturbations given only by air drag, based on the specific formulation of the TD88 density model, we will use the term the TD88 theory.

2.1 Areas of application

Hoots and France [16] state that in the future the role for semianalytical theories may disappear. Although they are relatively fast running on the computer, as the analytical methods do, they cannot give comparable physical insight into the character of the motion due to various perturbations. On the other hand, the unprecedented increase in computational power drives the numerical integration methods to be available for almost all satellite orbits computation, at least as regards the satellite cataloguing purposes, which is the context of the article cited.

The STOAG theory may be applied in situations, where

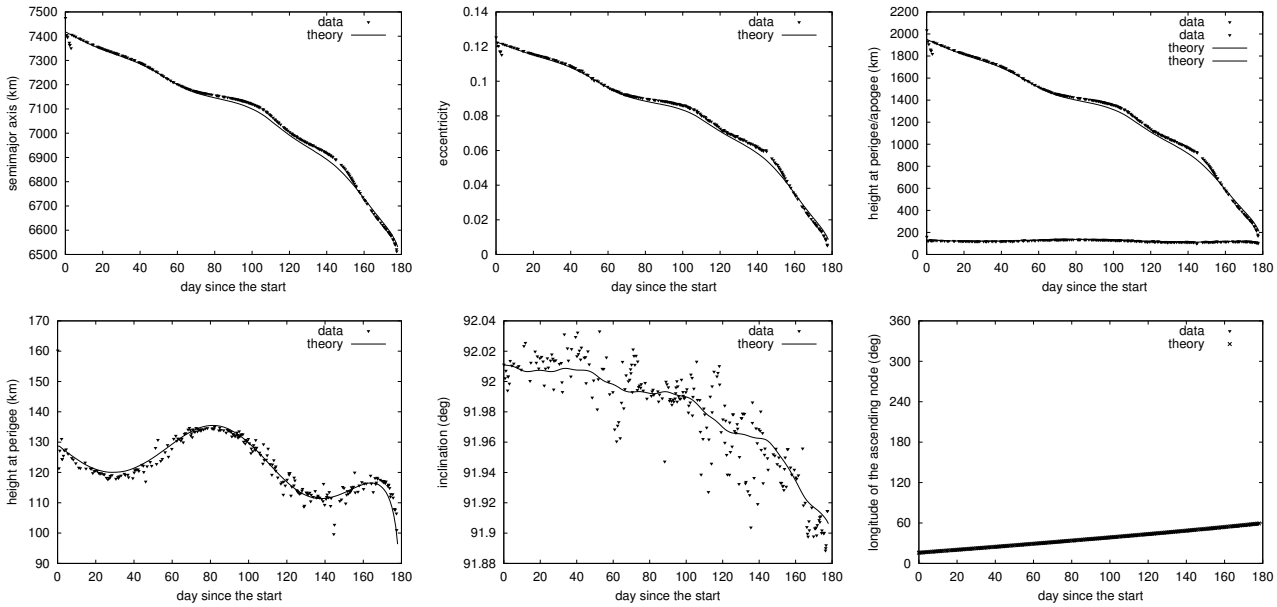

Fig. 2. Satellite Cannonball 2 (released on 7 Aug. 1971, d = 0,65 m, m = 364 kg).

one needs a quick orbital propagator for LEO objects, which are significantly influenced by air drag, but undergo the long-term gravitational variations as well (e.g. mission planning, lifetime prediction, space debris dynamics). Compared to the analytical theories including air drag [e.g. 13, 17], the STOAG theory embraces the dynamics of the thermosphere via the measured (or predicted) solar activity indices. In section 4 we will show a practical example for mission planning, where using STOAG one can investigate lots of possible mission scenarios, tested with respect to the required lifetime and other orbital characteristics. To validate the STOAG theory (and more specifically the TD88 model and theory) we compared its predictions with passive spherical satellites flown in the past, when the solar activity indices were known and the deviations of the "predicted" and measured orbital elements come from the theory itself. Each time we started with only one initial set of orbital elements, which was propagated further on. The unavoidable uncertainties (or possible errors) in the initial orbital elements and/or in the physical characteristics of a satellite were relegated to the "C_D-induced" confidence interval, which we defined to quantify the uncertainty in our prediction of the orbital elements evolution. Such examples of validation are in sections 3 and 4, for more detailed discussion and other example satellites see [2].

Note to the reader. – Owing to the limited extent of this text, for mathematical definition and other implementation comments regarding the STOAG theory, we kindly ask the reader to refer to the more extensive paper [2].

3 COMPARISON WITH SATELLITE ORBITS

GFZ-1 (1995-020A). – GFZ-1 was a small passive spherical satellite released from MIR on 19 April 1995 into a nearly spherical orbit at an initial altitude of 390 km with the inclination of 51.6°, and decayed after 1525 days (for more information, see http://op.gfz-potsdam.de/gfz1/gfz1.html). In Fig. 1 are the modelled and measured data, which were obtained from the two-line element (TLE) series with J_2-induced short perturbations removed. The steady decrease in the semimajor axis is caused by the action of air drag, leading finally to the decay of the satellite from its orbit. The theoretical curves labelled by $C_D = 2.09$ and $C_D = 2.31$ show the a priori assessed uncertainty band in the predicted orbital element evolution, corresponding to $C_D = 2.2 \pm 5$ % [for details, see 2]. The model curve labelled with $C_D = 2.12$ was obtained as a global "best fit" with respect to the lifetime of the satellite (this value of C_D is used for the theoretical curves in other panels of Fig. 1). The inclination of GFZ-1 displays the overall decrease caused by air drag, the long-period oscillations are predominantly due to the lunisolar perturbations. Finally, due to the low eccentricity the nonsingular elements were used throughout the whole lifetime, which couple the gravitational and drag perturbations in the eccentricity and argument of perigee (the bottom two graphs in Fig. 1). The theory shows quite well the variations due to the odd zonal harmonics of the geopotential, leading to the libration of the argument of perigee around 90°, combined with the action of the drag that modifies the amplitude of the variations.

Cannonball 2 (1971-067C). – Cannonball 2 was a high-density satellite designed to study the thermosphere at very low altitudes, in the last days of flight it descended down to 100–110 km, to the bottom of the thermosphere. To be able to use the TD88 theory at these heights, we nonlinearly fitted the free parameters of TD88 to 2.5 million of the MSIS-86 model densities within the height range 100–150 km. In Fig. 2 we draw the TLE (with the short-period gravitational perturbations removed) together with the theoretical curves. In this case the global

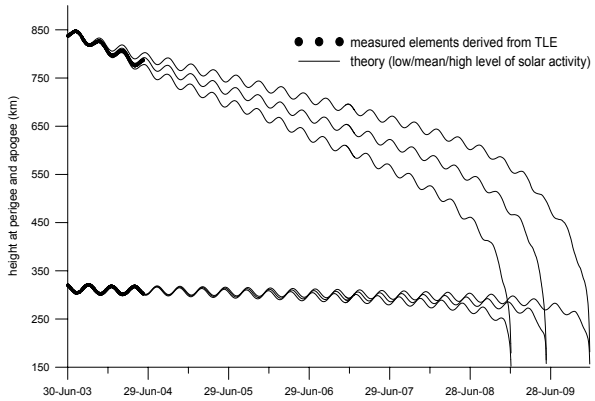

Fig. 3. Long-term orbital and lifetime prediction for Mimosa.

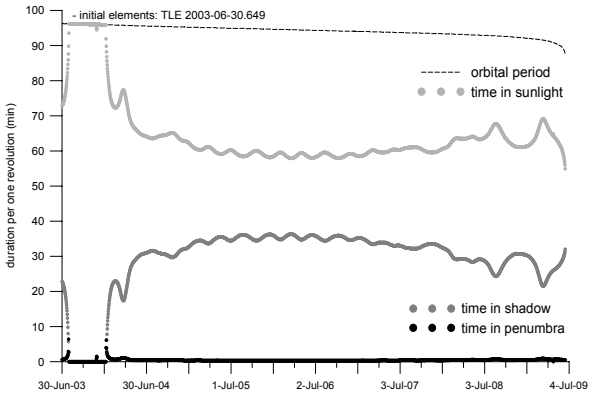

Fig. 4. Prediction of lighting conditions on the Mimosa orbit.

best-fit drag coefficient is lower, $C_D = 1.68$, which is in agreement with the fact that near its perigee the satellite moved at the boundary between the free molecular flow regime and the hypersonic continuum flow, where the C_D coefficient is reduced from about 2.3 to about 1.0 [18].

4 APPLICATION TO PROJECT MIMOSA

MIMOSA(2003-031B) is a small Czech scientific satellite with a sensitive microaccelerometer on its board, whose aim is to measure the nongravitational forces acting on LEO satellites [19]. The satellite was launched on 30 June 2003 to a nearly sunsynchronous orbit with 320 km at perigee and 840 km at apogee, inclined at 96.8° to the equator.

4.1 Mission planning

We used the STOAG theory during the preparatory phase of the project. The relatively quick computation enabled us to investigate many configurations of the initial orbital elements and to search for a set optimizing the lifetime and other orbital requirements. An illustration of these simulations is in Table 1. In this case we were interested in finding the optimum lifetime with regard to that of the instruments aboard, together with the orbit scanning the altitude profile of the thermosphere down to the lower heights. For a given orbit we could very quickly calculate the long-term evolution of the orbital elements (Fig. 3) or study the lighting conditions (Fig. 4). These are examples of using the long-term, mean orbital elements that make the output of the STOAG theory.

In accordance with the overview in section 1.1, we can analytically add the short-term periodics to the mean STOAG elements, so that we obtain the approximate motion of the satellite. Namely, to study the "full" motion of the satellite, we completed the linearly interpolated mean elements with the J_2-induced short-period gravitational perturbations. In this way, we could have an idea of the passage times of Mimosa over the ground station (Fig. 5) and what are the lighting conditions during the passages (not in Fig. 5).

Tab. 1. Model predictions for the lifetime of Mimosa. Three lines with the same initial heights at perigee h_p and apogee h_a represent minimum, mean and maximum level of the modelled solar activity.

Initial height		Lifetime	After 2 yrs		After 4 yrs	
h_p(km)	h_a(km)	(years)	h_p	h_a	h_p	h_a
280	700	2.2	243.8	345.3	.0	.0
		1.7	.0	.0	.0	.0
		1.4	.0	.0	.0	.0
	800	3.2	261.6	566.1	.0	.0
		2.6	253.5	482.8	.0	.0
		2.0	210.3	269.2	.0	.0
	900	4.4	269.0	700.4	247.9	416.1
		3.5	263.5	647.4	.0	.0
		2.9	255.7	574.5	.0	.0
300	700	3.5	283.8	529.7	.0	.0
		2.8	276.4	470.8	.0	.0
		2.2	255.4	359.6	.0	.0
	800	5.1	287.8	663.7	280.6	497.1
		4.2	283.7	626.9	254.0	342.8
		3.4	278.3	578.0	.0	.0
	900	6.1	297.6	772.1	285.1	663.1
		5.6	294.0	743.1	275.9	599.7
		5.0	289.2	707.5	268.2	514.4
320	700	5.2	306.9	596.3	302.9	464.7
		4.3	303.1	566.7	270.4	361.3
		3.5	297.7	526.6	.0	.0
	800	6.4	312.8	710.2	302.6	632.5
		5.9	309.8	688.3	298.5	584.6
		5.4	306.0	661.3	295.0	525.7
	900	7.4	323.7	809.4	322.2	739.0
		6.8	321.2	790.7	315.7	708.1
		6.4	318.0	768.4	307.6	675.6

4.2 First year of flight

In Fig. 6 we draw the long-period TLE and the theoretical curves for two versions of STOAG – with and without the lunisolar perturbations, both using $C_D = 2.11$ (best-fit with respect to the overall decrease in the semimajor axis after one year). While in the semimajor axis, and in other orbital elements, the lunisolar perturbations are insignificant in relation to the other geopotential-induced perturbations, the inclination of Mimosa shows an increasing trend, which is caused by the lunisolar forces – contrary to the steady decrease induced by air drag (the curve in

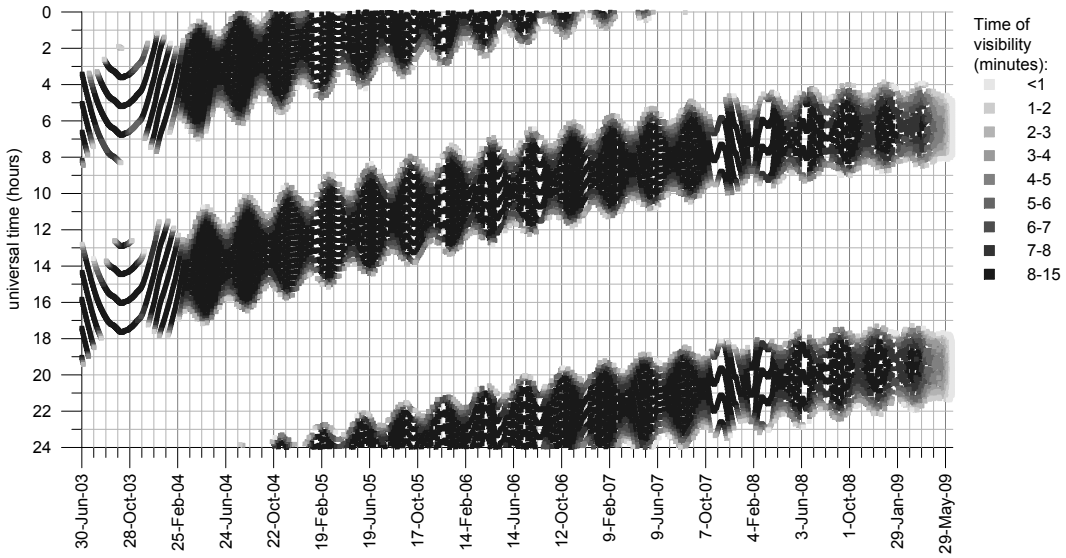

Fig. 5. Prediction of visibility for the passages of Mimosa over the ground station at Panska Ves, Czech Republic. The markers indicate the moment, when Mimosa culminates for a given passage. Initial elements: TLE 2003-06-30 15:34:33.

Fig. 6 labelled as "theory without lunisol. pert."). This is not surprising, as the orbit is nearly sunsynchronous (conf. the slowly changing passage times in Fig. 5), and the STOAG theory demonstrates this increasing trend in inclination in an approximate manner, probably due to the simplified lunisolar perturbation model and other uncertainties (e.g. in TLE).

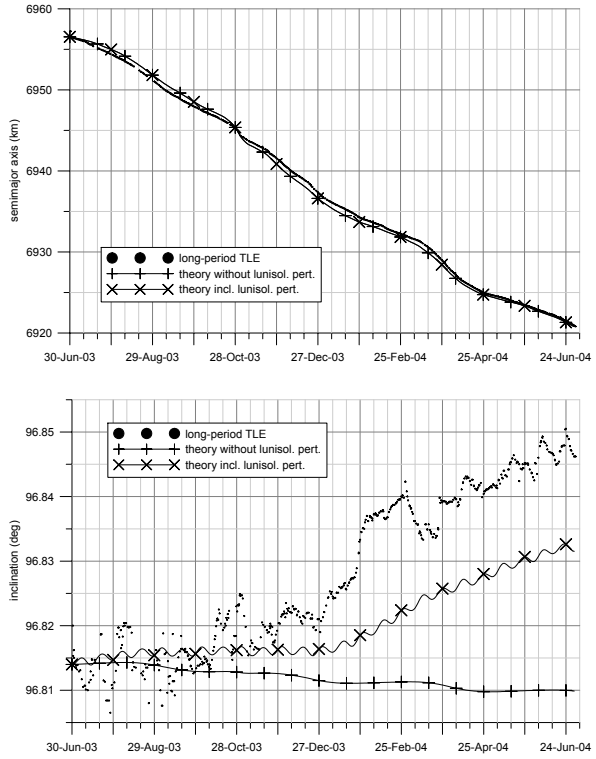

Fig. 6. Evolution of the orbital elements of Mimosa during the first year of flight: semimajor axis and inclination.

Note. – The online calculation as well as the Fortran 77 code of the STOAG theory are available on the Web site http://www.asu.cas.cz/˜bezdek/density_therm/pohtd/.

ACKNOWLEDGEMENTS

This work was supported by a grant no. ME 488 from the Ministry of Education of the Czech Republic.

REFERENCES

1. Hoots, F. R., France, R. G.: An analytic satellite theory using gravity and a dynamic atmosphere. *Celest. Mech. 40*, 1–18, 1987.
2. Bezděk, A., Vokrouhlický, D.: Semianalytic theory of motion for close-Earth spherical satellites including drag and gravitational perturbations. *Planet. Sp. Sci.*, in print. Preprint version http://www.asu.cas.cz/˜bezdek/density_therm/papers/, 2004.
3. de Lafontaine, J., Hughes, P.: An Analytic Version of Jacchia's 1977 Model Atmosphere. *Celes. Mech.* 29, 3–26, 1983.
4. Gill, E.: Smooth Bi-Polynomial Interpolation of Jacchia 1971 Atmospheric Densities For Efficient Satellite Drag Computation. DLR-GSOC IB 96-1, 1996.
5. ECSS. *Space engineering. Space environment.* European Cooperation for Space Standardization, ESA-ESTEC Publications Division, ECSS-E-10-04A, 2000.
6. Marcos, F. A.: AFRL Satellite Drag Research. The 2002 Core Technologies for Space Systems Conference, Colorado Springs, Colorado, November 19–21, 2002.
7. Sehnal, L.: Theory of the motion of an artificial satellite in the Earth atmosphere. *Adv. Space Res.* 10(3-4), 297–301, 1990.

8. Sehnal, L., Pospíšilová, L.: Lifetime of the ROHINI A satellite. *Bull. Astron. Inst. Czechosl.* 42, 295–297, 1991.
9. Sehnal, L.: Thermospheric total density model TD. Bull. *Astron. Inst. Czechosl.* 39, 120–127, 1988.
10. Sehnal, L., Pospíšilová, L.: Thermospheric model TD88. Preprint No. 67 of the Astron. Inst. Czechosl. Acad. Sci., 1988.
11. Sehnal, L.: Comparison of the thermosphere total density model TD 88 with CIRA 86, *Adv. Space Res.* 10(6), 27–31, 1990.
12. Barlier, F., Berger, F., Falin, J.L., Kockarts, G., Thuillier, G.: A thermospheric model based on satellite drag data. *Ann. Geophys.* 34, 9–24, 1978.
13. King-Hele, D. G.: *Theory of satellite orbits in an atmosphere*. Butterworth, London, 1964.
14. Zarrouati, O.: *Trajectoires Spatiales*. Cepaudes-Editions, Toulouse, 1987.
15. Estes, R.: On the analytic lunar and solar perturbations of a near Earth satellite. *Celest. Mech.* 10, 253–276, 1974.
16. Hoots, F. R., France, R. G.: The future of artificial satellite theories. *Celest. Mech.* 66, 51–60, 1997.
17. Brouwer, D., Hori, G.: Theoretical evaluation of atmospheric drag effects in the motion of an artificial satellite. *Astron. J.* 66, 193–225, 1961.
18. Montenbruck, O., Gill, E.: *Satellite Orbits*. Springer-Verlag, Berlin, 2001.
19. Peřestý, R., Sehnal, L., Pospíšilová, L.: Project Mimosa – final stage of the satellite fabrication. *Acta Astronautica* 52, 819–823, 2003.